

ARL 70-0128
JULY 1970



AD 712412

Aerospace Research Laboratories

MEASUREMENT OF SOUND VELOCITY IN A SOLID-GAS MIXTURE

B. N. TURMAN, 2ndLt., USAF

ENERGETICS RESEARCH LABORATORY

PROJECT NO. 7116

This document has been approved for public release and sale;
its distribution is unlimited

AIR FORCE SYSTEMS COMMAND

United States Air Force

Approved for Release by NSA on 05-08-2014 pursuant to E.O. 13526

NOTICES

When Government drawings, specifications, or other data are used for any purpose other than in connection with a definitely related Government procurement operation, the United States Government thereby incurs no responsibility nor any obligation whatsoever; and the fact that the Government may have formulated, furnished, or in any way supplied the said drawings, specifications, or other data, is not to be regarded by implication or otherwise as in any manner licensing the holder or any other person or corporation, or conveying any rights or permission to manufacture, use, or sell any patented invention that may in any way be related thereto.

Agencies of the Department of Defense, qualified contractors and other government agencies may obtain copies from the

Defense Documentation Center
Cameron Station
Alexandria, Virginia 22314

This document has been released to the

CLEARINGHOUSE
U. S. Department of Commerce
Springfield, Virginia 22151

for sale to the public.

SEARCHED	INDEXED
SERIALIZED	FILED
OCT 1970	
FBI - VIRGINIA	

Copies of ARL Technical Documentary Reports should not be returned to Aerospace Research Laboratories unless return is required by security considerations, contractual obligations or notices on a specified document.

ARL 70-0128

**MEASUREMENT OF SOUND VELOCITY
IN A SOLID-GAS MIXTURE**

B. N. TURMAN

ENERGETICS RESEARCH LABORATORY

JULY 1970

PROJECT NO. 7116

This document has been approved for public release
and sale; its distribution is unlimited.

AEROSPACE RESEARCH LABORATORIES
AIR FORCE SYSTEMS COMMAND
UNITED STATES AIR FORCE
WRIGHT-PATTERSON AIR FORCE BASE, OHIO 45433

FOREWORD

This report deals with part of a continuing in-house research program on multi-component flow phenomena conducted in the Energetics Research Laboratory under Project No. 7116, "Energy Conversion Research".

The author wishes to express appreciation for the discussion he has had with Dr. Hans J.P. von Ohain, Dr. Brian Quinn, and Mr. Siegfried Hasinger. Mr. Brian Hausfeld is to be thanked for his assistance in installing and operating the experimental apparatus.

ABSTRACT

Velocity of sound through a two-component (solid-gas) medium was measured as a function of solid particle concentration. A method was devised in which phase angle between a sound source signal and microphone signal could be measured as a function of solid particle density in the apparatus. Acoustical theory provided the necessary relationship between phase angle, density, and sound velocity. Sound velocity in the two-component medium was measured over a particle volume fraction range from 10^{-4} to 0.5. The possibility of using this technique as a diagnostic instrument is discussed.

TABLE OF CONTENTS

SECTION		PAGE
I	INTRODUCTION	1
II	DISCUSSION OF EXPERIMENT	5
III	DATA ANALYSIS	10
IV	CONCLUSIONS	16
V	REFERENCES	20
VI	APPENDIX A - SPEED OF SOUND THROUGH SUSPENDED POWDER	22
VII	APPENDIX B - ACOUSTIC IMPEDANCE AND THE EQUIVALENT CIRCUIT	28

LIST OF FIGURES

Figures	Page
1. The Acoustical System	33
2. The Complete Equivalent Circuit	34
3. Simplified Equivalent Circuit	34
4. Time Shifts as Displayed on Oscilloscope	35
5. Measured Time Shift as Function of Particle Volume Fraction	36
6. Experimental and Theoretical Determination of Sound Velocity as Function of Particle Volume Fraction	37
7. Ratio of Specific Heats as Function of Particle Volume Fraction	38
8. Comparison of Exact and Approximate Calculation of Sound Velocity as Function of Particle Volume Fraction	39

LIST OF SYMBOLS

a	=	tube radius
C_p	=	heat capacity of gas at constant pressure
C_v	=	heat capacity of gas at constant volume
C_s	=	heat capacity of solid particle
c	=	local speed of sound
c_o	=	speed of sound in particle free air
h_p	=	specific heat of gas at constant pressure
h_s	=	specific heat of solid
I	=	equivalent electric current
L	=	acoustic inductance
l	=	length of tube
P	=	pressure
Q	=	heat energy
R	=	acoustic resistance
r_m	=	ratio of solid density to gas density (ρ_p/ρ_g)
S	=	cross-sectional area
Δt	=	time increment
V	=	volume
V_p	=	volume occupied by particles
Z	=	acoustic impedance

β	=	ratio of local speed of sound to free air speed or sound (c/c_0)
Γ	=	ratio of specific heats for gas-solid mixture
γ	=	ratio of specific heats for pure gas (C_v/C_p)
δ	=	density variation due to sound wave
ϵ	=	void fraction (ratio of gas volume to total volume)
η	=	volume fraction of solid particles ($1-\epsilon$)
λ	=	wavelength of sound wave
ν	=	frequency of sound wave
ξ	=	displacement of gas due to sound wave
ρ_g	=	mass density of gas
ρ_p	=	particle mass density
ϕ	=	phase angle between driving signal and microphone signal
ϕ_0	=	initial phase angle
ω	=	angular frequency of sound wave

I. INTRODUCTION

Studies of sound propagation through multi-component media are of interest for a variety of reasons. A better understanding of the mechanics of multi-component flow can be obtained from analysis of sound propagation through the multi-component medium, both from direct experimental results and from comparison of experimental and theoretical predictions. Experimental and theoretical results indicate that sound velocity in multi-component media is dependent on particle concentration, which is of course important in determining Mach number in the flow. Acoustic instability phenomena are of direct interest to feasibility studies of the colloid core reactor concept (Ref. 1). Many of the diagnostic techniques presently employed in the study of multi-component flow are at a rather rudimentary level, and certain acoustic processes offer promise as diagnostic tools.

A considerable amount of effort has been devoted to the investigation of shock waves in multi-component media. The first analytical work in this area was done by Carrier (Ref. 2), and Rudinger extended this analysis with calculations of shock characteristics in two-phase flows (Ref. 3, 4, 5).

Manuscript released June 1970 by the author for publication as an ARL Technical Report.

The results showed that three distinct regions exist in the shock: the frozen flow zone, where gas-particle transport processes (drag and heat transfer) are negligible; the relaxation zone, where gas flow and particle flow interact; and the equilibrium zone where normal equilibrium flow is again established. In the frozen flow zone, the main expansion shock propagates at the shock velocity in clean gas, while the particles are essentially unaffected. The equilibrium wave propagates at a velocity that is dependent on the particle concentration, and consequently the Mach number of the two-phase flow is dependent on this parameter. Experimental work by Eddington (Ref. 6) has confirmed these predictions. Using water droplet-air mixtures, he has shown that shock phenomena occurring in single phase supersonic gas flow is duplicated in the two-phase flow, with appropriately modified specific heat ratio, density, and sound velocity.

The problem of sound velocity in mixed-phase media has been the subject of a number of investigations. Sound velocity in various two-phase media have been calculated: phase combinations include gas bubbles in a liquid medium (Ref. 7), solid particles in a liquid medium (Ref. 8), and

solid/liquid particles in a gaseous medium (Ref. 5). Ultrasonic resonance has been used to verify calculations of sonic speed in solid-liquid mixtures (Ref. 8, 9), and shock studies have verified calculations concerned with liquid-gas flow (Ref. 6).

The experiment described in this report is a determination of the sound velocity through a mixture of air and moderately large solid particles (glass spheres of around 40 μ diameter). Maintaining a suspension of these particles in an acoustic resonance tube (the technique used in Ref. 8), for sufficient time to complete the measurement is difficult; therefore, an alternate technique is used. The solid particles are allowed to fall through a vertical tube, essentially at terminal velocity. This tube is part of an acoustic network containing a driving source (loud speaker), a receiver (microphone) and an acoustic impedance (connecting tubes). Phase difference between the driving signal and microphone signal is measured as a function of particle concentration and the relation between phase difference, particle concentration and sound velocity through the powder mixture is derived. The data are compared with calculated values of sound velocity as a function of particle concentration.

The measurements of phase difference versus particle concentration suggest a possible use of this technique in monitoring particle concentration in multi-component flow. This application will be discussed more fully in Section IV.

II. DISCUSSION OF EXPERIMENT

The purpose of this experiment was to measure the speed of sound through a mixture of moderate sized particles and air. Solid glass spheres, with mean diameter around 40 microns and mass density of 2.35 gm/cm^3 , were chosen for the experiment. Particle size and density were dictated by a desire to relate the results of the measurement to investigations currently being conducted by this laboratory into the nature of multi-component vortex flow. The resonance technique employed in Ref. 8 is probably the most accurate means of measuring sound velocity. That method, however, was not well suited for this experiment because of the difficulty encountered in maintaining a stationary suspension of such large particles. A different technique was devised, and is explained in the following text.

Details of the acoustical system are shown in Fig. 1. Sound waves generated by a loud speaker are transmitted through the tube on the left to a T intersection. A portion of the sound signal continues through the tube on the right and is detected by a microphone placed at the end of the tube. The vertical tube in Fig. 1 acts as a second transmission line connected in parallel with the transmission line to the microphone. As explained in Appendix B, an acoustical network

can be reduced to the more familiar electrical circuit form by definition of an acoustical impedance. Fig. 2 and 3 show the analogous electrical circuit corresponding to the acoustical system of Fig. 1.

Fig 2 is the complete circuit, showing the driving voltage V applied to the loud speaker, the transformation from electrical energy to acoustic energy accomplished by the loud speaker (denoted by a "black box" τ), acoustic impedances of the transmission tubes (Z_o , Z_c , and Z_p), acoustic impedance of the microphone (Z_m), and finally the conversion from acoustic to electrical energy at the microphone (τ). Under certain conditions, as discussed in Appendix B, this complete circuit can be approximated by the simpler form shown in Fig. 3. The acoustic impedance of the vertical tube in Fig. 1 is denoted by Z_p , acoustic impedance of the transmission tube to the microphone is Z_c , and the acoustic impedance of the microphone is assumed to be purely resistive (R). The crux of the experiment is the measurement of phase angle between the A. C. signal driving the loud speaker and the signal received by the microphone. From Fig. 3, this phase angle is equivalent to the phase angle between the total current I and the

current flowing to the microphone, I_2 . The relationship between phase angle and the circuit elements R , Z_c , and Z_p is derived in Appendix B.

Solid particles were introduced into the vertical tube through the funnel shown in Fig. 1. A flow diffuser (a cluster of short, small diameter tubes placed at the top of the vertical tube) provided uniform powder flow across the tube cross-section. The glass spheres fell through the tube at terminal velocity (approximately 10 cm/sec), and uniform density was maintained along the length of the tube with constant powder flow rate out of the funnel. As shown in Appendix B, the impedance Z_p is dependent on the density of the air column, ρ , and the local sound velocity, c . By measuring particle concentration simultaneously with the phase angle between microphone and loud speaker signals, the sound velocity was determined as a function of particle concentration.

A dual beam oscilloscope was used to display both the microphone signal and the loud speaker signal. The speaker driving signal, supplied by a pulse generator operating at a frequency of 800 Hz, triggered both beams of the oscilloscope, so that the phase angle between driving signal and microphone signal could be read directly from the oscilloscope. The phase shift produced by the addition of solid

particles in the vertical tube was determined by measuring the displacement of the microphone signal along the time axis. Large magnifications of both oscilloscope axes were used in order to facilitate the measurement of the time shift. Fig. 4 shows an example of the measurement: the peak of the initial microphone signal (no powder flow) is superimposed on the shifted signal resulting from powder flow in the vertical tube. The time increment between the two peaks was used to determine phase shift.

Particle density in the powder stream was obtained by two different methods: light absorption for low density measurement, and mass flow rate for high density values. In the light absorption method, the powder flow was positioned between a light source and photometer; the decrease in light intensity caused by the flow of solid particles was used to calculate the number density of particles. For high flow density, the length of time required for a specified mass of powder to flow through the tube was used, along with the terminal velocity, to determine particle concentration. In the overlap region (around $\eta = .01$), both methods were used to insure compatibility of the two sets of data. Fig. 5

is a plot of time increment Δt versus particle volume fraction (η), where the particle volume fraction is just percentage of total volume occupied by solid particles, and is proportional to particle mass concentration.

III. DATA ANALYSIS

In essence, two quantities were measured in this experiment: the density of powder flowing in the powder tube, and the phase shift of the microphone signal associated with the powder density. The phase shift was measured on an oscilloscope by observing the displacement of the microphone signal along the time axis, as described in Section II, and shown in Fig. 4. Time increment is related to change in phase angle by

$$\Delta t = \frac{(\phi - \phi_0)}{2\pi\nu} \quad (1)$$

with ϕ denoting the new phase angle between speaker signal and microphone signal, ϕ_0 is the phase angle with no added powder, and ν is frequency.

The relation between phase angle and acoustic parameters is delineated in Appendix B. Specifically, Eq. (B21)

$$\tan \phi = \frac{L_c R_p / \omega - L_p R / \omega}{R_p^2 / \omega^2 + L_p^2 + R R_p / \omega^2 + L_p L_c} \quad (2)$$

L_c , L_p and R_p refer to the circuit elements of Fig. 3 and are functions of acoustical parameters: R must be determined

experimentally. L_c is a reasonably simple function, Eq.

(B.14):

$$L_c = \frac{\rho c}{\omega} \cot \frac{\omega l}{c} \quad (3)$$

Since ρ and c represent conditions in the free air of the microphone cavity and l is length of tube, L_c is a constant in the experiment. With the appropriate values ($l = 25$ cm, $\omega = 5 \times 10^3$ radians/sec) this impedance is

$$L_c = - .01 \text{ dyne-sec/cm}^3 \quad (4)$$

The two quantities relating to powder tube impedance are more complicated. As derived in Appendix B, Eq. (B15)

$$R_p = 2\pi^2 \rho c \left(\frac{a}{\lambda}\right)^2 \frac{1 + \tan^2 2\pi l_p / \lambda}{1 + 4\pi^4 (a/\lambda)^4 \tan^2 2\pi l_p / \lambda} \quad (5)$$

a is tube radius, λ is wavelength, and $l_p = l + \frac{8a}{3\pi}$

With the values $a = 2.5$ cm, $\lambda = 40.5$ cm (corresponding length in free air), $l_p = 87$ cm

$$R_p / \omega = 1.87 \beta \rho \quad (6)$$

with $\beta = c / c_0$; $c_0 =$ speed of sound in free air.

The inductive term is

$$L_p = - \frac{\rho c}{\omega} \frac{\tan 2\pi l_p / \lambda - 4\pi^4 (R/\lambda)^4 \tan 2\pi l_p / \lambda}{1 + 4\pi^4 (R/\lambda)^4 \tan^2 2\pi l_p / \lambda} \quad (7)$$

Upon substitution of the appropriate values in Eq. (7), again with the free air wave length, the inductive term is

$$L_p = -8.95 \beta \rho \quad (8)$$

Eq. (2) can now be written as

$$\tan \phi = \frac{8.95 R/\omega - .019}{82.5 \beta \rho + .089 + 1.87 R/\omega} \quad (9)$$

With no powder in the powder tube, the air density is 10^{-3} gm/cm^3 , and $\beta=1$. The phase angle for this condition was found to be .94 radian. Putting these values into Eq. (9) yields the value:

$$R/\omega = .04 \text{ dyne-sec/cm}^3 \quad (10)$$

Finally, the phase angle is related to density and sound speed by the function

$$\tan \phi = \frac{.004}{\beta \rho + .002} \quad (11)$$

Figure. 5 shows experimental measurements of time shift Δt as a function of powder density. Dots on this curve represent density values obtained from the light absorption technique, while crosses refer to data from the mass flow rate method. (For a complete discussion of these techniques, refer to Section II). The solid curve is calculated from Eq. (11), assuming $\beta=1$. The calculated curve approaches experimental results in the limits of low volume fraction and high volume fraction, but between those limits a large discrepancy exists. Assuming this discrepancy is due to the function $\beta(\eta)$, Eq. (11) can be applied to the experimental points in Fig. 5 to calculate sound velocity. This result is shown in Fig. 6, with the theoretical function derived in Appendix A shown as a solid curve.

Agreement between experimental and theoretical sound velocity is fairly good. The random variations that are apparent in Fig. 6 are due mainly to experimental errors in measuring powder density, as errors involved in measuring phase shift should be negligible. Some of the errors inherent in the density measurements are as follows: non-uniform density through the powder tube, irregularities in powder feed (which would give variation of instantaneous powder

density that would not be seen from integrated powder flow rate measurement), and the slow response time of the photomultiplier (of the order of .5 sec) which would mask rapid fluctuations in powder density. There is a better agreement between theoretical values and data taken with flow rate determination of density because each of these points is actually an average of 5 independent measurements: thus most of the random spread has been removed from these data. The point at $\eta = .4$ shows a significantly large deviation from the calculated curve. At such large particle concentration, particle-particle interaction may be of importance, noticeably altering the terminal settling velocity for the particles. Also, calculation of β becomes quite sensitive to error in measuring time shift, Δt , as well as initial phase angle, ϕ_0 , at high particle concentration. Therefore, systematic error may be introduced in this region, and less confidence should be placed on the data at high concentrations.

A systematic trend below the theoretical curve seems to be in evidence in the vicinity of a volume fraction of .005. This trend may be the result of an approximation made in arriving at Eq. (11). The constants in Eq. (11) are really

combinations of L_p (from Eq. (7) and (8)) and R_p (Eq. (5) and (6)). The approximation involved is the neglect of the dependence of L_p and R_p on wavelength. The complex dependence makes a complete analysis of these parameters both complicated and sensitive to errors in β . The sharp variations in R_p and L_p with wavelength occur due to resonances between an incoming sound wave and a wave reflected from the open end of the tube. The introduction of powder into the tube may smooth out these sharp resonances, as each particle can act as a source of reflected sound. Then some averaged value of R_p and L_p would be appropriate. This effect may explain the surprisingly good agreement between theory and experiment obtained by completely neglecting wavelength variation in the calculation of the parameters R_p and L_p .

IV. CONCLUSIONS

Results of this experiment indicate that the propagation velocity of sound in a solid-gas medium is dependent on the concentration of solids, and the sound velocity for highly loaded mixtures may be only a small fraction of the pure gas sonic velocity. The theoretical calculation of velocity ratio, β , in Fig. 6, shows a minimum value of .04 at a particle volume fraction of 0.5, while experimental data reaches a minimum value at a slightly lower volume fraction. Beyond this point, β increases rapidly with increasing particle load. According to Eq. (A35), β becomes infinite at $\epsilon=0$, but in reality this limit should be the sound velocity in the solid material, around 5000 m/sec for glass. This minor discrepancy is due to the neglect of the compressibility of the solid particle. The higher relative velocity obtained experimentally at $\eta = .4$ may be the result of sound transmission through clusters of solid particles. At such high particle concentration, local irregularities in mixture density may approach the solid material density, and sound transmission through this region would proceed at a much higher rate than through the bulk distribution. No conclusive statement can be made in this regard at present,

however, because of the uncertainty involved in this datum point (refer to the comments in Section III).

In deriving the expression for sound velocity in the solid-gas mixture, it was tacitly assumed that particle inertial effects were negligible; i.e., it was assumed that solid particles were moved by the pressure wave identically with the gas, so that density of the medium could be taken as the sum of densities of the two components. The general agreement between experimental data and the theoretical curve seems to justify this assumption, but with particles of larger diameter, or higher density, inertial effects may become important.

Analysis of many multi-component flow phenomena would be significantly simplified if one could consider the inhomogeneous medium as a perfect gas, with some modification of the appropriate parameters. As an example of this simplification, Eq. (A20) can be used to obtain an expression for β in the solid-gas mixture. The modified specific heat ratio Γ is substituted for γ , and the density of the mixture is taken as $\epsilon\rho_g + (1-\epsilon)\rho_p$. The result for the ratio of sound velocity in the mixture to that in the perfect gas is

$$\beta^* = \sqrt{\frac{\Gamma/\gamma}{\epsilon + (1-\epsilon)r_m}} \quad (12)$$

Comparison of this result with the more exacting derivation in Eq. (A35) shows that the two results differ only by a factor $\epsilon^{-1/2}$. These two functions are plotted in Fig. 8: Eq (12) is shown as a solid curve, and Eq.(A35) is shown with a broken curve. Since $\epsilon \approx 1$ for small values of η ($\eta \approx 1 - \epsilon$), the two curves are practically equivalent up to a solid volume fraction of 0.01. Thus it appears that these simplifying assumptions can be used safely for particle volume fraction lower than about .01.

Vortex flows with sub-micron size condensation particles have been studied by Fletcher, et al (Ref. 13). Volume fraction of liquid in these experiments was on the order of 10^{-4} , so that sound velocity should be around 90% of the value for pure gas, and Mach number of the flow would be about 10% higher than the corresponding value for pure gas flow. Investigations into the nature of vortex flows with high solid particle loading are currently being conducted in this laboratory. Solid volume fraction as high as 0.1 has been obtained in this work, with tangential velocities considerably higher than the 20 m/sec sonic velocity predicted by Fig. 6. Study of these flow conditions with high loading may provide further insight into the dependence of sound velocity on particle concentration.

With only minor modification, the experimental apparatus described in this report could be used as a diagnostic instrument for measuring density in linear flows. The powder flow to be measured would be directed through the vertical tube of Fig. 1, and the resulting phase shift converted to particle density (or volume fraction) with the calibration curve in Fig. 5. One problem associated with this technique may be interference from noise generated by the powder flow. More study must be given this point to find a suitable operating frequency with little extraneous noise, or develop a noise filtering system. Of particular interest to this laboratory is the development of diagnostic equipment suitable for use with swirl chambers such as that described in Ref. 13. Basically, these chambers are large diameter cylinders with axial vortex flows. Noise level during operation of these chambers is rather high, so noise interference would be a major problem for the phase shift measurement. The particle concentration obtained from the phase shift measurement would probably be an average over the entire vortex flow, as the whole chamber would be incorporated in the acoustic system. However, Ref. 14 indicates that at sufficiently high flow rate, sound attenuation perpendicular to the flow becomes strong. Under these conditions, localized density measurement with the phase shift experiment may be possible.

V. REFERENCES

1. Staff, Westinghouse Astronuclear Laboratory, "Engineering Study of Colloid Fueled Nuclear Rocket," Aerospace Research Laboratories technical report ARL 69-0234 (1969).
2. Carrier, G.F., "Shock Waves in a Dusty Gas," Journal of Fluid Mechanics, 4, 376 (1958).
3. Rudinger, George, "Some Properties of Shock Relaxation in Gas Flows Carrying Small Particles," Physics of Fluids, 7, 658 (1964).
4. Rudinger, George, and Chang, Angela, "Analysis of Nonsteady Two-Phase Flow," Physics of Fluids, 7, 1747 (1964).
5. Rudinger, George, "Some Effects of Finite Particle Volume on the Dynamics of Gas-Particle Mixtures," AIAA Journal, 3, 1217 (1965).
6. Eddington, Robert B., "Investigation of Supersonic Phenomena in a Two-Phase (Liquid-Gas) Tunnel," AIAA Journal, 8, 65 (1970).
7. Tangren, R.F., Dodge, C.H., and Siefert, H.S., "Compressibility Effects in Two-Phase Flow," Journal of Applied Physics, 20, 637 (1949).
8. Urick, R.J., "A Sound Velocity Method for Determining the Compressibility of Finely Divided Substances," Journal of Applied Physics, 18, 983 (1947).
9. Hampton, Loyd D., "Acoustic Properties of Sediments," Journal of the Acoustical Society of America, 42, 882 (1967).
10. Morse, Philip M., "Vibration and Sound," 2nd Edition, McGraw-Hill Book Company, Inc., New York (1948).
11. Beranek, Leo L., "Acoustic Measurements," John Wiley & Sons, Inc., New York (1949).
12. Page, Leigh, and Adams, Norman Ilakey Jr., "Principles of Electricity," 3rd edition, D. Van Nostrand Company, Inc., New York (1958).
13. Fletcher, Eugene C., Gyarmathy, George, and Hasinger, Siegfried, "Separation of Submicron Condensate Particles in a Vortex Chamber," Aerospace Research Laboratories technical report ARL 66-0218 (1966).

14. Pridmore-Brown, D.C., "Sound Propagation in a Fluid Flowing Through an Attenuating Duct," Journal of Fluid Mechanics, 4, 393 (1958).

VI. APPENDIX A

Speed of Sound Through Suspended Powder

In this section the equation of propagation of a pressure wave through a suspended powder is developed. In order to compare the result directly with the pure gas solution, the classical derivation for a homogeneous gas is first presented (taken largely from the derivation by Morse, Ref. 10).

We consider the propagation of a plane pressure wave through a cylindrical tube of cross-sectional area S . $\xi(x, t)$ denotes displacement of gas due to the wave, P is pressure, and ρ is gas density.

The total mass within the volume Sdx is

$$dm = \rho S dx \tag{A1}$$

This quantity is conserved as the pressure wave passes. As the waves pass, one bounding plane moves a distance $\xi(x)$, while the other plane moves a distance $\xi(x+dx)$. The volume element changes to a value

$$S[dx - \xi(x) + \xi(x+dx)] = S dx + S \frac{\partial \xi}{\partial x} dx \tag{A2}$$

The density is taken to be

$$\rho(x, t) = \rho_0(1+\delta) \tag{A3}$$

where δ is considered to be much less than 1. With conservation of the mass in Eq. (A1) we have

$$dm = \rho_0 S dx = S \rho_0 (1+\delta) \left(1 + \frac{\partial \xi}{\partial x}\right) dx \tag{A4}$$

This equation gives the result, to first order, that

$$\delta = -\frac{\partial \xi}{\partial x} \quad (\text{A5})$$

The equation of state for a perfect gas is

$$PV = RT \quad (\text{A6})$$

A temperature differential dT gives

$$RdT = PdV + VdP \quad (\text{A7})$$

and dividing Eq. (A7) by (A6) yields

$$\frac{dT}{T} = \frac{dP}{P} + \frac{dV}{V} \quad (\text{A8})$$

Heat capacity at constant volume, C_v , is defined as the amount of heat, dQ , absorbed per unit temperature increment with constant volume

$$C_v = \left(\frac{dQ}{dT} \right)_v \text{ constant} = \frac{\partial Q}{\partial P} \left(\frac{dP}{dT} \right)_v \text{ constant} \quad (\text{A9})$$

now $\left(\frac{dP}{dT} \right)_v = P/T$, so we have

$$C_v = \frac{\partial Q}{\partial P} \frac{P}{T} \quad (\text{A10})$$

In a similar manner we derive the heat capacity at constant pressure:

$$C_p = \frac{\partial Q}{\partial V} \frac{V}{T} \quad (\text{A11})$$

When both P and V are allowed to change, the heat change is

$$dQ = \frac{\partial Q}{\partial V} dV + \frac{\partial Q}{\partial P} dP \quad (A12)$$

and combination with Eq. (A10) and (A11) give

$$dQ = T \left(C_p \frac{dV}{V} + C_v \frac{dP}{P} \right) \quad (A13)$$

Propagation of a sound wave through air is very nearly adiabatic, that is $dQ = 0$. Therefore

$$C_p \frac{dV}{V} = -C_v \frac{dP}{P} \quad (A14)$$

Writing the pressure term as $P = P_0 + p$, and noting that Eq.

(A2) shows the volume change to be $S \frac{\partial \xi}{\partial x} dx$, we obtain the equation

$$C_p \frac{\partial \xi}{\partial x} = -C_v \frac{p}{P_0} \quad (A15)$$

and with

$$\gamma = C_p / C_v$$

$$p = \gamma P_0 \delta \quad (A16)$$

The force acting on the volume element at x is

$$[P_0 + p(x)]S - [P_0 + p(x+dx)]S = -S \frac{\partial P}{\partial x} dx \quad (A17)$$

With mass ρSdx and acceleration $\frac{\partial^2 \xi}{\partial t^2}$, the equation of motion is

$$\rho \frac{\partial^2 \xi}{\partial t^2} = - \frac{\partial P}{\partial x} \quad (A18)$$

Combining Equations (A18), (A16) and (A5) we have the two wave equations

$$\frac{\partial^2 \xi}{\partial t^2} = \frac{\gamma P_0}{\rho_0} \frac{\partial^2 \xi}{\partial x^2} \quad (A19)$$

$$\frac{\partial^2 P}{\partial t^2} = \frac{\gamma P_0}{\rho} \frac{\partial^2 P}{\partial x^2}$$

These equations indicate that pressure and particle velocity are propagated by wave motion with the phase velocity

$$c_0 = \sqrt{\frac{\gamma P_0}{\rho_0}} \quad (A20)$$

The result in Eq. (A20) is the sonic speed in a homogeneous gas: now we shall revise the derivation by assuming that solid particles are suspended in the gas, with void fractions being defined as the ratio of gas volume to total volume, and particle volume fraction η defined as the ratio of particle volume to total volume. The ratio of particle density ρ_p to gas density ρ_g is r_m .

The total mass in the test volume Sdx is now given by

$$\begin{aligned} dm &= Sdx[(1-\epsilon)\rho_g + \epsilon\rho_p] \\ dm &= r_m[1-\epsilon \frac{r_m-1}{r_m}] \rho_g Sdx \end{aligned} \quad (A21)$$

The equation of state for the solid-gas mixture will be written as

$$P(V-V_p) = RT \quad (A22)$$

with the result corresponding to Eq. (B8) of

$$\begin{aligned} \frac{dP}{P} + \frac{dV}{V-V_p} &= \frac{dT}{T} \\ \text{or} \quad \frac{dP}{P} + \frac{dV}{\epsilon V} &= \frac{dT}{T} \end{aligned} \quad (A23)$$

The heat capacity calculations are changed somewhat with the addition of powder, since the solid heat capacity C_s must now be considered.

At constant volume, the amount of heat added per unit rise of temperature

is $(dQ)_v = (C_v + C_s) dT$ (A24)

and from Eq. (A23),

$$\begin{aligned} \frac{\partial Q}{\partial P} \left(\frac{dP}{dT} \right)_v &= C_v + C_s \\ \frac{\partial Q}{\partial P} &= (C_v + C_s) \frac{T}{P} \end{aligned} \quad (A25)$$

Similarly,

$$(dQ)_p = (C_p + C_s) dT$$

which leads to the result

$$\frac{\partial Q}{\partial V} = (C_p + C_s) \frac{T}{\epsilon V} \quad (A26)$$

When both P and V vary, the heat addition is

$$\begin{aligned} dQ &= \frac{\partial Q}{\partial V} dV + \frac{\partial Q}{\partial P} dP \\ dQ &= [(C_p + C_s) \frac{dV}{\epsilon V} + (C_v + C_s) \frac{dP}{P}] T \end{aligned} \quad (A27)$$

and the adiabatic restriction yields

$$\frac{dV}{\epsilon V} = - \frac{C_v + C_s}{C_p + C_s} \frac{dP}{P} \quad (A28)$$

and with the result of Eq. (A2), we have

$$\begin{aligned} \frac{\partial \xi}{\partial x} &= -\epsilon \frac{C_v + C_s}{C_p + C_s} \frac{P}{P_0} \\ \frac{\partial \xi}{\partial x} &= -\epsilon \frac{1 + C_s/C_p}{1 + C_s/C_p} \frac{P}{P_0} \end{aligned} \quad (A29)$$

If h_p = heat capacity of gas at constant pressure, and h_s = heat capacity of solid

$$\begin{aligned} C_s &= \rho_p (1 - \epsilon) h_s \\ C_p &= \rho_g \epsilon h_p \\ B &\equiv C_s/C_p = r_m \frac{1 - \epsilon}{\epsilon} \frac{h_s}{h_p} \end{aligned} \quad (A30)$$

and Eq. (A29) can be expressed in the simpler form

$$\frac{\partial \xi}{\partial x} = -\epsilon \frac{1 + B}{1 + B} \frac{P}{P_0} \quad (A31)$$

with

$$\begin{aligned} P &= \Gamma P_0 \delta \\ \Gamma &= \frac{1 + B}{1 + \gamma + B} \end{aligned} \quad (A32)$$

The equation of motion, analogous to Eq. (A18) is

$$\left[1 - \epsilon \frac{r_m - 1}{r_m}\right] r_m \rho_g \frac{\partial^2 \xi}{\partial t^2} = - \frac{\partial p}{\partial x} \quad (\text{A33})$$

and we have the wave equation

$$\frac{\partial^2 \xi}{\partial t^2} = \frac{\Gamma P_0}{\epsilon r_m \rho_g \left[1 - \epsilon \frac{r_m - 1}{r_m}\right]} \frac{\partial^2 \xi}{\partial x^2} \quad (\text{A34})$$

The phase velocity is therefore

$$c = \sqrt{\frac{\Gamma P_0}{\epsilon r_m \left[1 - \epsilon \frac{r_m - 1}{r_m}\right] \rho_g}}$$

$$\beta \equiv c/c_0 = \sqrt{\frac{\Gamma/\gamma}{r_m \epsilon \left[1 - \epsilon \frac{r_m - 1}{r_m}\right]}} \quad (\text{A35})$$

$$\beta = \sqrt{\frac{\Gamma/\gamma}{\epsilon \left[\epsilon + (1 - \epsilon) r_m\right]}} \quad (\text{A36})$$

$$\Gamma/\gamma = \frac{1 + B}{1 + B\gamma} \quad (\text{A37})$$

For the particular case of solid glass spheres suspended in air, we have the following parameters:

$$r_m = 1.9 \times 10^3$$

$$\gamma = 1.4$$

$$h_g = 0.12 \quad (\text{A38})$$

$$h_p = 0.22$$

$$B = 1 \times 10^3 \frac{1 - \epsilon}{\epsilon} \quad (\text{A39})$$

$$B/\gamma = 715 \frac{1 - \epsilon}{\epsilon}$$

The function β is plotted in Fig. 6, and Γ is plotted in Fig. 7.

VII. APPENDIX B

Acoustic Impedance and the Equivalent Circuit

In electrical circuit theory, a quantity called the electrical impedance of a circuit element is defined as the ratio of applied voltage to current, and it may be a complex number. Well known rules exist for calculating the effect of combinations of individual circuit elements (e. g., series-parallel combinations of resistors, capacitors, or coils) so that electrical characteristics of complicated circuits can be deduced by proper application of those rules. In this appendix, the acoustical impedance is derived, enabling electrical circuit theory to be applied by analogy to acoustical network problems. The derivation is essentially taken from Morse, (Ref. 10).

The pressure p in the acoustical system will correspond to electrical voltage, particle velocity ξ corresponds to electrical current, and the acoustical impedance is therefore

$$Z = \frac{P}{\xi} \quad (B1)$$

Consider propagation of a sound wave through a tube of radius a and length l . As shown in Appendix A, pressure and particle displacement can both be expressed as wave functions. For a tube of finite length, a reflected wave as well as the primary wave will be present, so that pressure function will have the form

$$p = P_+ e^{ik(x-ct)} + P_- e^{-ik(x+ct)} \quad (B2)$$

P_+ is the magnitude of the primary wave, P_- is magnitude of reflected wave, c is the propagation velocity, $k = \omega/c$, and ω is propagation angular frequency. The complex number ρ is defined such that

$$P_-/P_+ = \rho \quad (B3)$$

Then

$$p(x) = P_+ e^{-\psi - i\omega t} \left(e^{\psi + ikx} - e^{-\psi - ikx} \right)$$

$$p(x) = 2P_+ e^{-\psi - i\omega t} \sinh \left(\psi + \frac{i\omega x}{c} \right) \quad (B4)$$

In a similar fashion, particle displacement can be written as

$$\xi(x) = P_+ K e^{-\psi - i\omega t} \left(e^{\psi + ikx} + e^{-\psi - ikx} \right) \quad (B5)$$

where the constant K must be determined.

From Eq. (A16) and (A20) (or equivalently Eq. (A31) and (A35) pressure and displacement are related by

$$p = -\rho c^2 \frac{\partial \xi}{\partial x}$$

Evaluation of this equation at $x=0$ gives the complex constant value

$$K = \frac{1}{\rho c \psi} \quad (B6)$$

Particle velocity is

$$\dot{\xi} = i \frac{P_+}{\rho c \omega} e^{-\psi - i\omega t} \left(e^{\psi + ikx} + e^{-\psi - ikx} \right) (-i\omega)$$

$$\dot{\xi} = \frac{2P_+}{\rho c} e^{-\psi - i\omega t} \cosh \left(\psi + \frac{i\omega x}{c} \right) \quad (B7)$$

Therefore, in accordance with Eq. (B1)

$$Z = \rho c \tanh \left(\psi + \frac{i\omega x}{c} \right) \quad (B8)$$

This equation will now be applied to two specific problems of interest, namely a calculation of acoustic impedance of a closed tube of length l , and an open tube of length l .

As mentioned previously, ψ may be complex. Therefore, let us define the quantity $\psi + \frac{i\omega x}{c} = \pi(a - ib)$ (B9)

$$a = \frac{1}{\pi} \operatorname{Re} \psi, \quad b = -\frac{1}{\pi} \operatorname{Im} \psi = \frac{\omega x}{\pi c}$$

The ratio of the magnitude of reflected wave to incident wave is $e^{-\operatorname{Re} \psi}$

Now suppose that the propagation tube is closed at $x=l$ by a rigid plate

Then the magnitudes of reflected and incident wave are equal, giving $a=0$

The impedance term reduces to

$$Z = \rho c \tanh(-i\pi b) = -i\rho c \tan\pi b \quad (\text{B10})$$

At $x = 1$, the impedance is infinite, requiring

$$b_1 = 1/2 = -\frac{1}{\pi} I_m \psi - \frac{\omega l}{\pi c} \quad (\text{B11})$$

or
$$-I_m \psi = \frac{\pi}{2} + \frac{\omega l}{c}$$

Then
$$b = 1/2 + \frac{\omega l}{\pi c} - \frac{\omega x}{\pi c}$$

The impedance of the closed tube at $x=0$ is therefore

$$Z_0 = -i\rho c \tan\left(\frac{\pi}{2} + \frac{\omega l}{c}\right)$$

or
$$Z_0 = i\rho c \cot\frac{\omega l}{c} \quad (\text{B12})$$

The derivation of impedance of an open tube is too lengthy for presentation here: reference should be made to Ref. 10 for details.

The acoustic impedance at the driving end, $x=0$, of an open tube of length l and radius a is given approximately by

$$Z_0 = -i\rho c \frac{\tan 2\pi l_p/\lambda + i2\pi^2(a/\lambda)^2}{1 - i2\pi^2(a/\lambda)^2 \tan 2\pi l_p/\lambda} \quad (\text{B13})$$

with
$$l_p = l + 8a/3\pi$$

The acoustic impedances derived above can now be applied to the acoustical system shown in Fig. 1. As outlined in Ref. 11, an equivalent electrical circuit can be constructed, and is shown in Fig. 2. Coupling between electrical and acoustical energy, as performed by both the loud speaker and microphone, is denoted by τ ; Z_m is mechanical impedance of microphone, and will be assumed purely resistive. Z_0 represents impedance of the tube connecting the loud speaker to the T section. Z_c is impedance of tube from T section to microphone, and Z_p is impedance of powder tube. The frequency was selected so that the phase shift resulting from Z_0 was π radians, and assuming equivalent reactance in coupling at the loud speaker and microphone, the equivalent circuit in Fig. 2 can be reduced to the circuit in Fig. 3,

with the stipulation that a phase lag of π radians is introduced in the signal generator.

From Eq. B12, the impedance Z_c (closed tube) is purely inductive, i. e.

$$Z_c = i\omega L_c \quad (B14)$$

$$L_c = \frac{\rho c}{\omega} \cot \frac{\omega l}{v}$$

Eq. B13 indicates that Z_p (open tube) is complicated: after some algebraic manipulation the impedance can be expressed in the simpler form

$$Z_p = R_p + i\omega L_p \quad (B15)$$

$$R_p = 2\pi^2 \rho c (a/\lambda)^2 \frac{1 + \tan^2 2\pi l_p/\lambda}{1 + 4\pi^4 (a/\lambda)^4 \tan^2 2\pi l_p/\lambda}$$

$$L_p = - \frac{\rho c}{\omega} \frac{\tan 2\pi l_p/\lambda - 4\pi^4 (a/\lambda)^4 \tan 2\pi l_p/\lambda}{1 + 4\pi^4 (a/\lambda)^4 \tan^2 2\pi l_p/\lambda}$$

Currents in the parallel circuits are divided such that

$$I_1 Z_p = I_2 (R + Z_c) \quad (B16)$$

$$I_1 (R_p + i\omega L_p) = I_2 (R + i\omega L_c)$$

$$(I_1 - I_2)(R_p + i\omega L_p) = I_2 (R + i\omega L_c) \quad (B17)$$

Rearrangement of terms leads to

$$\frac{I_2}{I_1} = \frac{R_p + i\omega L_p}{R + R_p + i\omega(L_c + L_p)} \quad (B18)$$

By multiplying both numerator and denominator by the complex conjugate of the denominator, the complex term in the denominator is removed, with the result

$$\frac{I_2}{I_1} = \frac{[(R+R_p)(R_p + \omega^2 L_p(L_c + L_p))] + i\omega[L_p(R+R_p) - R_p(L_c + L_p)]}{(R+R_p)^2 + \omega^2(L_c + L_p)^2} \quad (B19)$$

The phase angle ϕ between currents I_2 and I is obtained from the equation*

$$\tan\phi = - \frac{\text{Im}(I_2/I)}{\text{Re}(I_2/I)} \quad (\text{B20})$$

where of course Im denotes the imaginary portion of the function and Re the real part.

$$\tan\phi = - \frac{\omega[L_p(R+R_p) - R_p(L_c+L_p)]}{(R+R_p)R_p + \omega^2 L_p(L_c+L_p)}$$

or

$$\tan\phi = \frac{L_c R_p / \omega - L_p R / \omega}{R_p^2 / \omega^2 + L_p^2 + R R_p / \omega^2 + L_p L_c} \quad (\text{B21})$$

The phase angle ϕ represents the phase lag between currents I_2 and I , or equivalently the phase lag between speaker signal and microphone signal. Therefore Eq. (B21) is the relationship between the acoustical properties of the system and the measured phase angle required to complete the analysis of the experiment.

The functional forms of L_p , R_p , and L_c have been derived: only R remains to be determined. Since R is the microphone resistance and will contain acoustic as well as electrical terms, it is best determined experimentally, as is explained in the data analysis section.

*This formula differs from the standard relation given in texts on electrical circuit theory by the factor -1 (see for instance Ref. 12). The minus sign is due to a difference in writing the oscillating time dependence, which for standard electrical circuit theory is written as $e^{i\omega t}$, as compared to the form $e^{-i\omega t}$ used in this derivation. The result is a difference in sign for the phase lag ϕ .

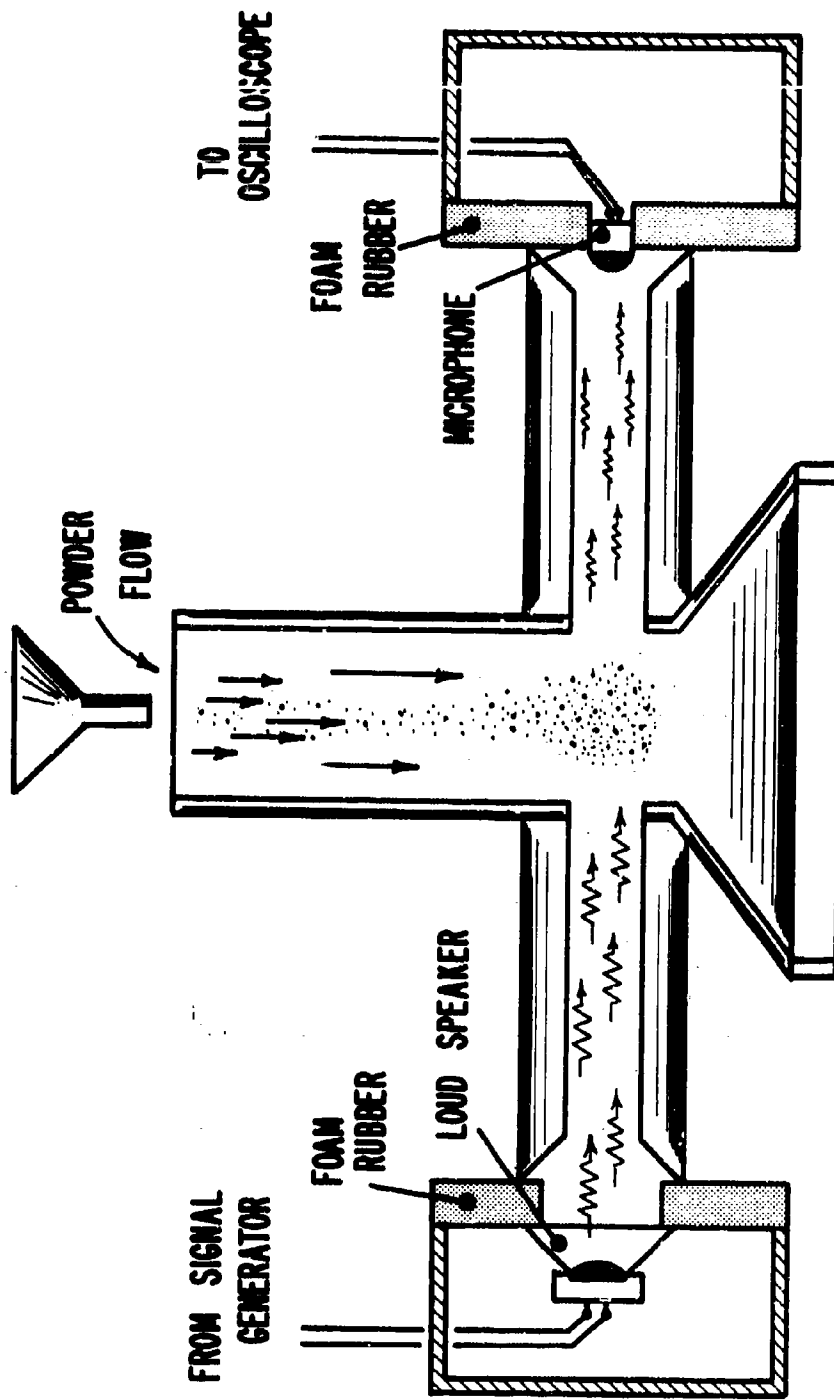


Figure 1. The Acoustical System

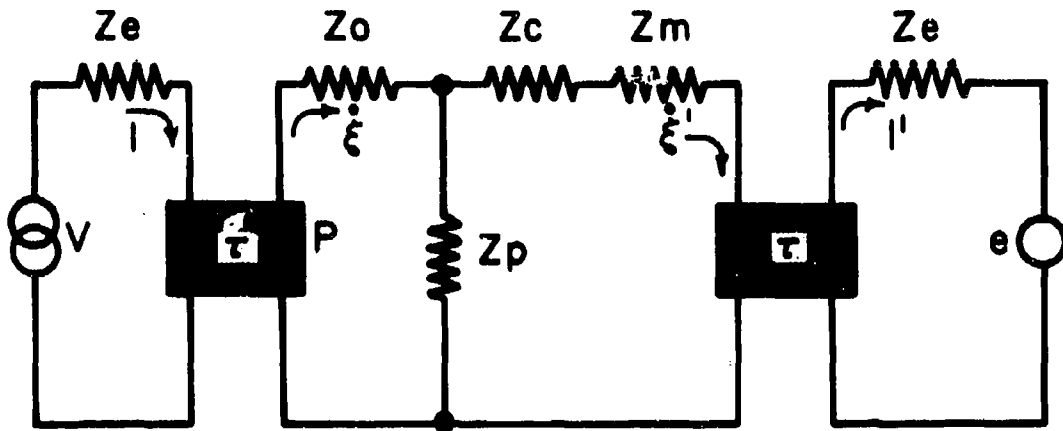


Figure 2. The Complete Equivalent Circuit

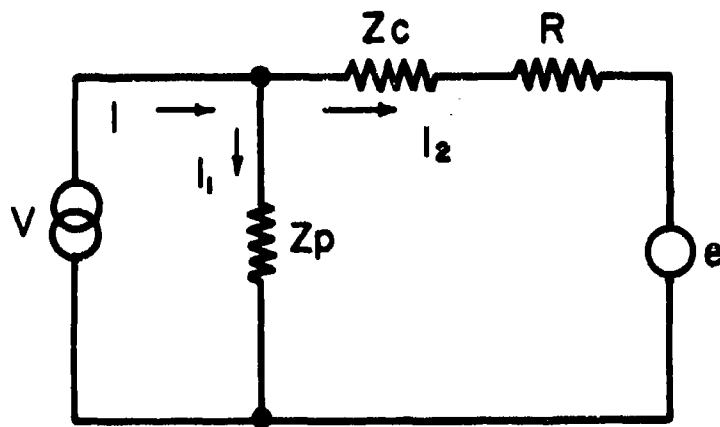
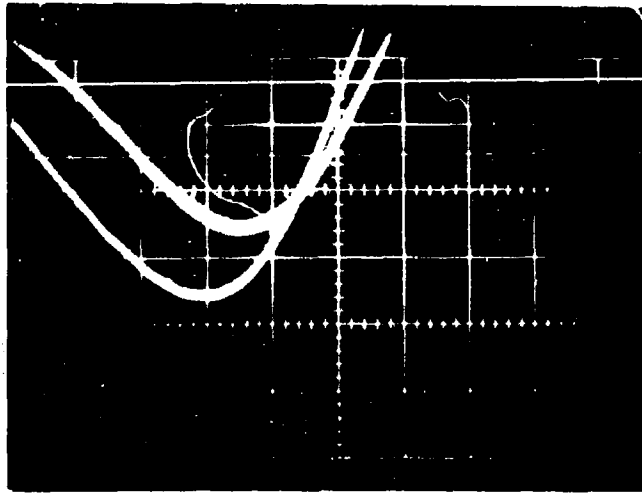
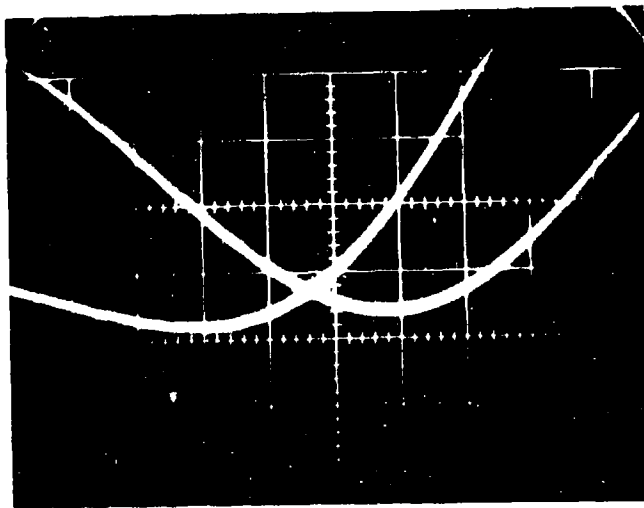


Figure 3. Simplified Equivalent Circuit



a. 100 micro-sec/cm time scale



b. 50 micro-sec/cm time scale

Figure 4. Time shifts as displayed on Oscilloscope

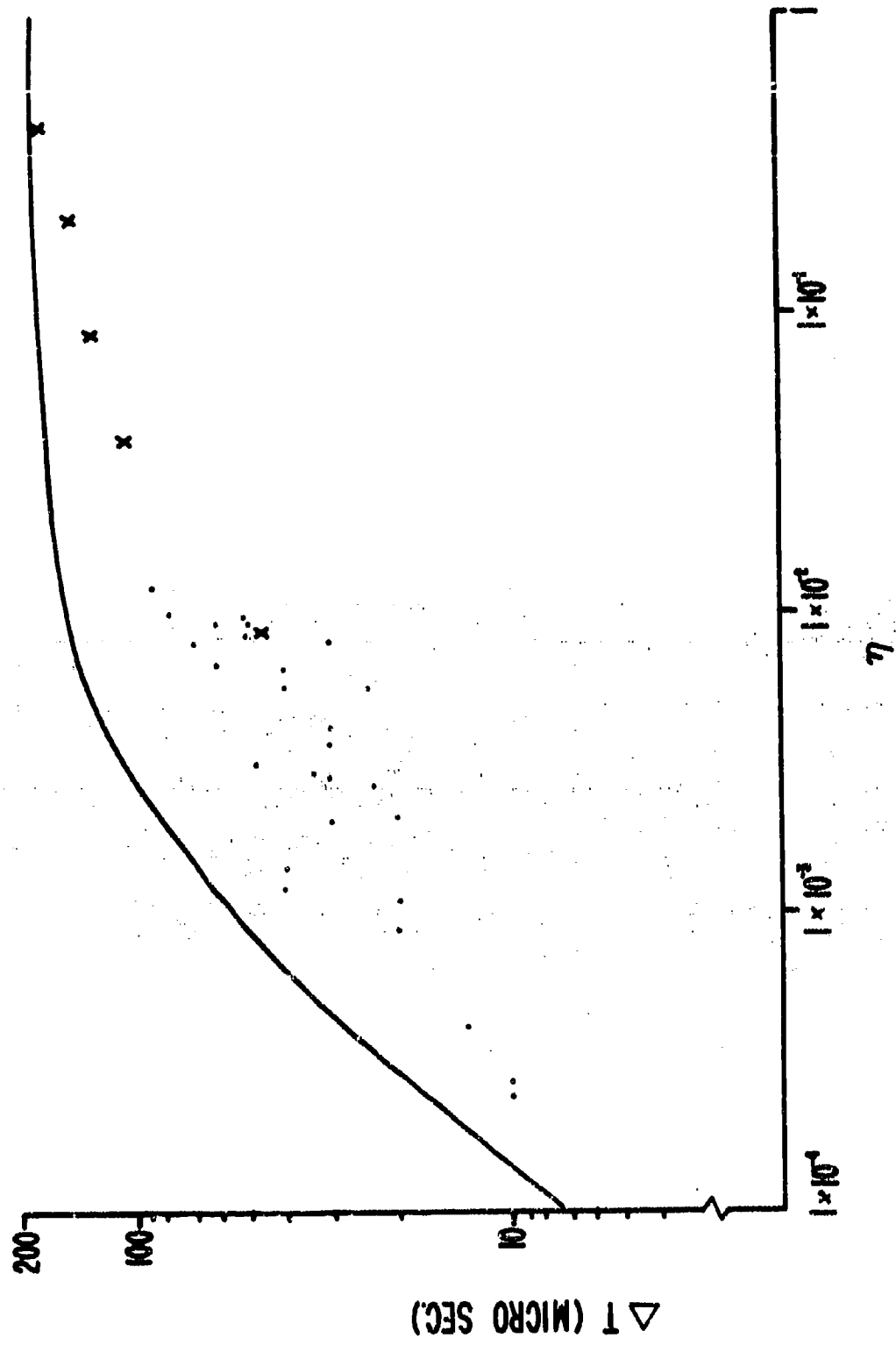


Figure 5. Measured Time Shift as Function of Particle Volume Fraction

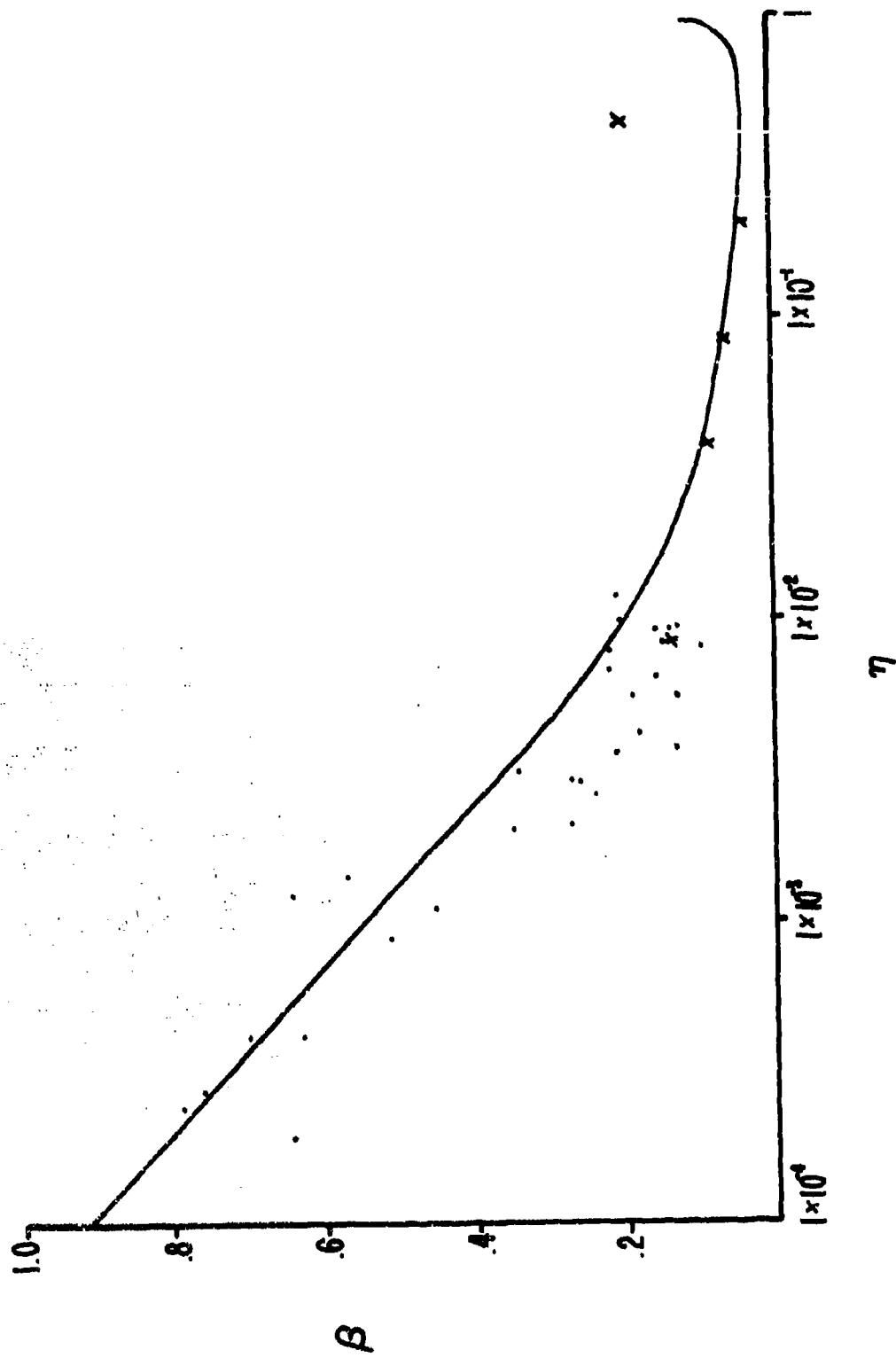


Figure 6. Experimental and Theoretical Determination of Sound Velocity as Function of Particle Volume Fraction

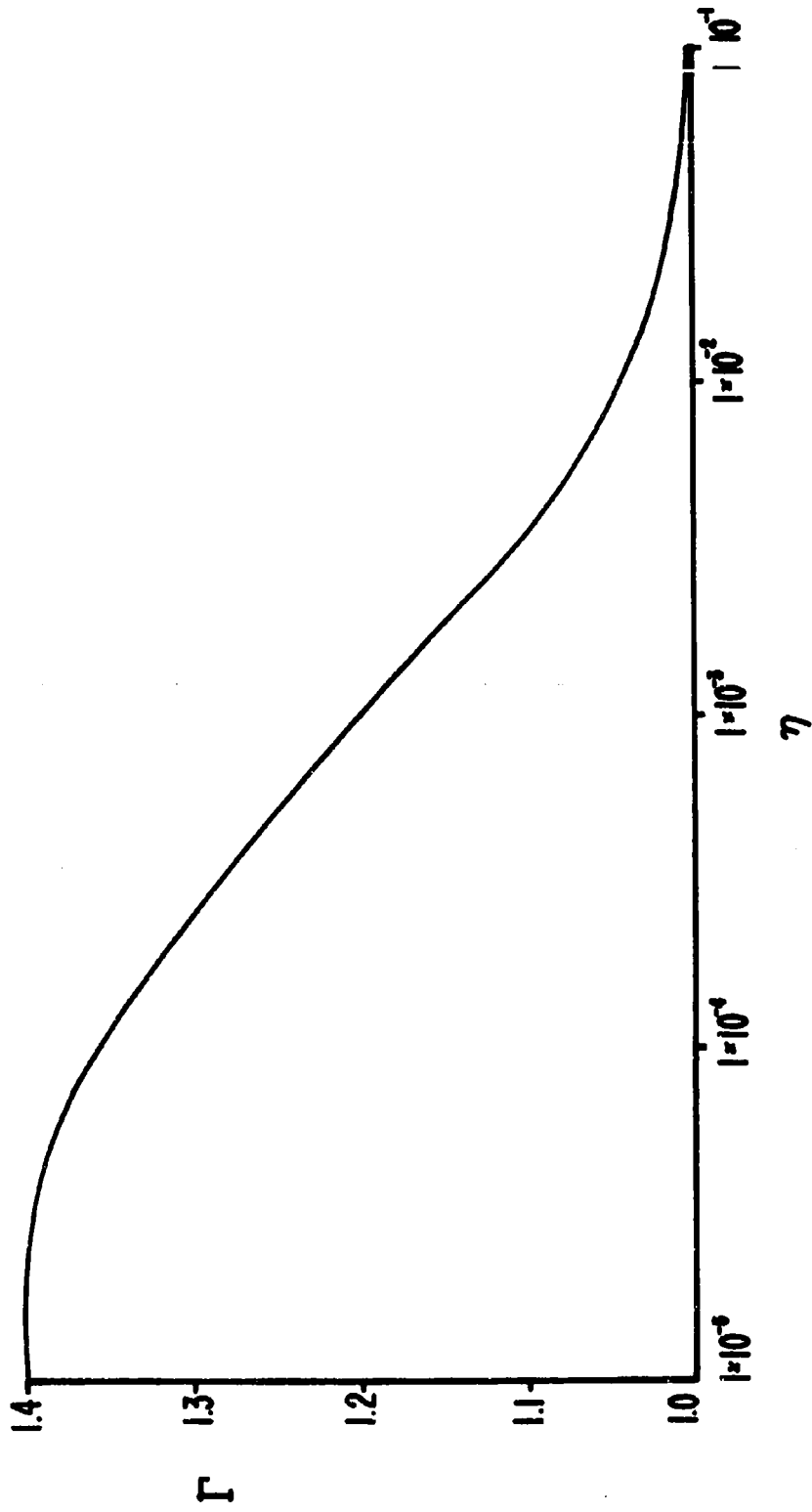


Figure 7. Ratio of Specific Heats as Function of Particle Volume Fraction

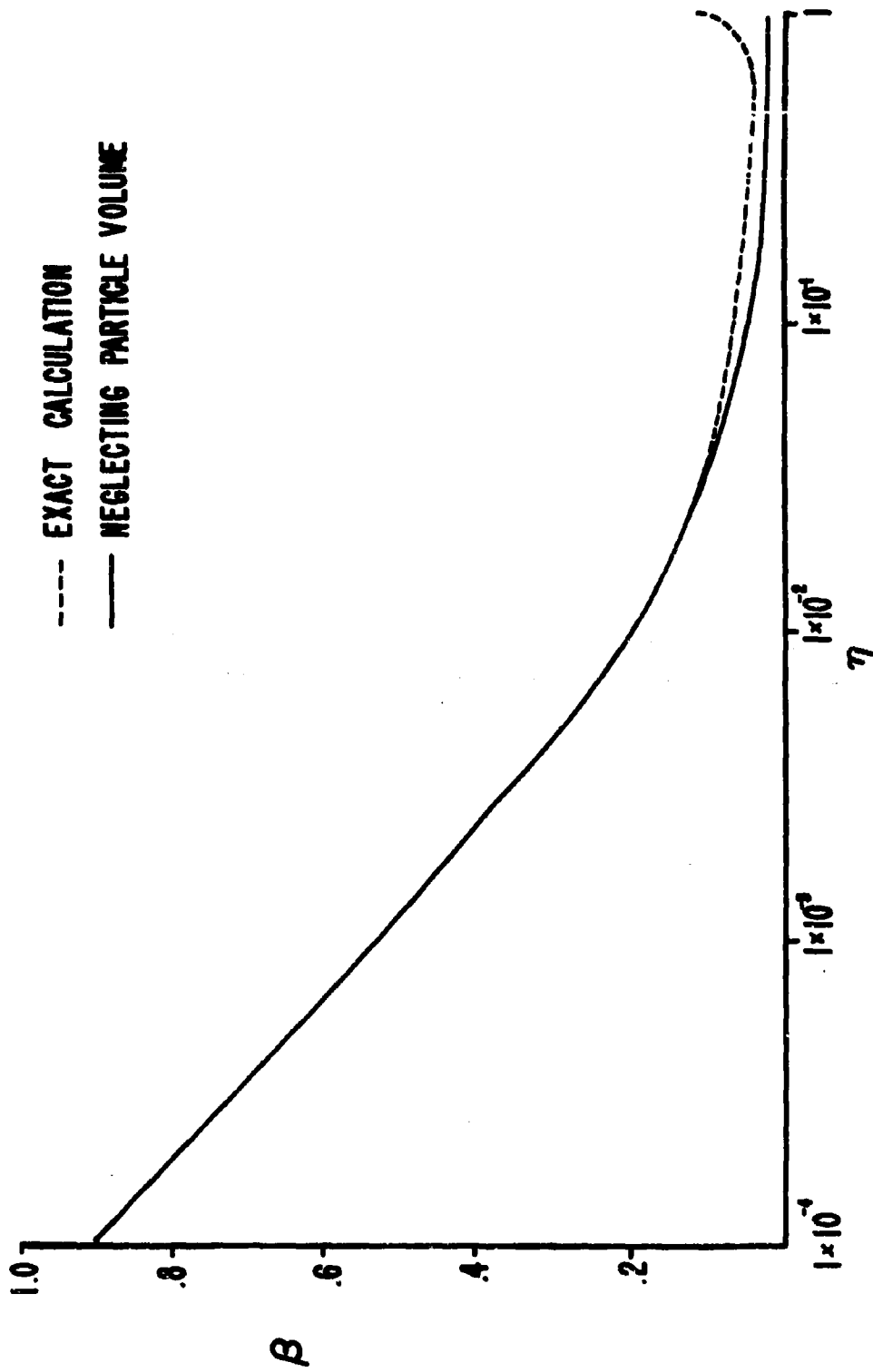


Figure 8. Comparison of Exact and Approximate Calculation of Sound Velocity as Function of particle Volume Fraction

~~Unclassified~~
Security Classification

DOCUMENT CONTROL DATA - R & D		
<i>(Security classification of title, body of abstract and indexing annotation must be entered when the overall report is classified)</i>		
1. ORIGINATING ACTIVITY (Corporate author) Aerospace Research Laboratories Energetics Research Laboratory (ARE) Wright-Patterson AFB, Ohio		2a. REPORT SECURITY CLASSIFICATION Unclassified
		2b. GROUP
3. REPORT TITLE "Measurement of Sound Velocity in a Solid-Gas Mixture"		
4. DESCRIPTIVE NOTES (Type of report and inclusive dates) Scientific. Final.		
5. AUTHOR(S) (First name, middle initial, last name) Turman, B.N.		
6. REPORT DATE July 1970	7a. TOTAL NO. OF PAGES 47	7b. NO. OF REFS 14
8a. CONTRACT NUMBER In-house Research		9a. ORIGINATOR'S REPORT NUMBER(S)
b. PROJECT NO 7116-0001		
c. DoD Element 61102F		9b. OTHER REPORT NO(S) (Any other numbers that may be assigned this report)
d. DOD Subelement 681308		ARL 70-0128
10. DISTRIBUTION STATEMENT 1. This document has been approved for public release and sale; its distribution is unlimited.		
11. SUPPLEMENTARY NOTES TECH OTHER		12. SPONSORING MILITARY ACTIVITY Aerospace Research Laboratories (ARE) Wright-Patterson AFB, Ohio
13. ABSTRACT Velocity of sound through a two-component (solid-gas) medium was measured as a function of solid particle concentration. A method was devised in which phase angle between a sound source signal and microphone signal could be measured as a function of solid particle density in the apparatus. Acoustical theory provided the necessary relationship between phase angle, density, and sound velocity. Sound velocity in the two-component medium was measured over a particle volume fraction range from 10^{-4} to 0.5. The possibility of using this technique as a diagnostic instrument is discussed.		

DD FORM 1473

Unclassified

Security Classification

Security Classification

KEY WORDS	LINK A		LINK B		LINK C	
	ROLE	WT	ROLE	WT	ROLE	WT
Sound Velocity Multi-component Flow Multi-component Flow Diagnostics						

Security Classification